Chemical Papers (2021) 75:9–25
https://doi.org/10.1007/s11696-020-01273-4

ORIGINAL PAPER

Combined experimental and theoretical investigation of optical and structural properties of poly aniline derivatives

Abdolreza Majidizadeh Fini[1] · Forough Kalantari Fotooh[1] · Mohammad Reza Nateghi[1] · Somayeh Shahi[1]

Received: 13 April 2020 / Accepted: 27 June 2020 / Published online: 7 July 2020

Abstract

The structure of poly aniline (PANI), poly para phenylenediamine (PpPDA), and poly benzidine (PBz) is strongly dependent on the synthesis conditions and procedure. For this reason there is an ambiguity in the proposed structure of the polymers in the literature. A density functional theory (DFT) calculation were performed to establish the structure of synthesized PANI, PpPDA, and PBz. Different structures were considered for each polymer and fully optimized. Then their electrical and optical properties were calculated. Experimental band gaps of studied polymers were obtained using cyclic voltammetry technique and compared with those calculated by DFT. Optical band gap was also obtained from UV–visible spectrum of each polymer dissolved in DMSO solvent. Optical band gap value obtained for aniline is 1.90 eV which is close to the experimental band gap value reported for emeraldine form of poly aniline. Comparing calculated and experimental HOMO–LUMO gaps decline the formation of benzoid (PPDA-a) and phenenzine (PPDA-b) structures during synthesis of PpPDA. However, the exact structure of PpPDA was recognized through comparing experimental and simulated optical properties. Calculated electronic and optical band gaps of phenanzine structure of synthesized benzidine (PBz-c) are close to those of experimental ones and are confirmed by the spectroscopic results. Obtained results show that theoretical calculations play an important role in the detection of complex polymer structures.

Keywords Poly aniline · Band gap · DFT calculations · Electrical and optical properties

Introduction

Nowadays conducting polymers such as PANI and its derivatives have attracted many attentions due to their well-defined nature and special optical and electrical properties (Bazito et al. 2008; Ćirić-Marjanović 2013; Nateghi and Savabieh 2014; Sapurina and Stejskal 2008; Stejskal et al. 2010). In recent years, aromatic diamines have been employed in the synthesis of new conjugated polymers to acquire materials which can exhibit better chemical functionality, mechanical and thermal properties than PANI (Li et al. 2002). It has been shown that a hybrid (polymer/inorganic) heterojunction device built on PANA-ES shows a photovoltaic performance which can be employed as a promised heterojunction solar cell (Al-Hossainy et al. 2018). Moreover, doped-poly (aniline-co-4-nitroaniline) thin films have shown reliable photovoltaic features (Al-Hossainy and Zoromba 2019). The most frequently used derivatives of aniline are phenylenediamines (PDA) that form polymers with lower conductivity and redox activity (Guimard et al. 2007; Li et al. 2002; Sestrem et al. 2009, 2010; Stejskal 2015; Yang and Liao 2012; Yang et al. 2014; Zoromba et al. 2018). These polymers have been studied more especially in biomedical applications with lower potential toxicity compared to aniline (Guimard et al. 2007). PpPDA nanofibers have shown high-efficiency effects on enhancing the fluorescence intensity of l-cysteine (l-Cys) (Yang and Liao 2012). Moreover, the combination of Fe_3O_4 with PpPDA leads to high photo catalytic activity in the degradation of the dyes under both ultraviolet and visible radiation (Yang et al. 2014).

The structures of these polymers and consequently their electronic properties are very susceptible to their polymerization procedure. Poly aniline has different structures, which depends on their synthesis method. Oxidation of aniline under acidic conditions produces the emeraldine salt with

✉ Forough Kalantari Fotooh
f-kalantari-f@iauyazd.ac.ir

✉ Mohammad Reza Nateghi
mnateghi@iauyazd.ac.ir

[1] Department of Chemistry, Yazd Branch, Islamic Azad University, Yazd, Iran

equal number of secondary amine groups and imine nitrogen atoms (Stejskal and Gilbert 2002; Stejskal et al. 1996). The emeraldine form of poly aniline can be chemically or electrochemically oxidized to pernigraniline (Stejskal et al. 1996). Some studies suggest that the pernigraniline salts are conducting (Bazito et al. 2008). The reduction of emeraldine yields leucoemeraldine form with non-conducting behavior. Various polymer structures can be considered for poly para-PDA. The poly aniline-like chain is probably the most obvious structure for this polymer (Li et al. 2013; Min et al. 2011; Wu et al. 1996). At higher oxidation concentration, a phenanzine like ladder structure is produced (Amer and Young 2013; Baibarac et al. 2011; Cheng et al. 2006; Muthirulan and Rajendran 2012; Sayyah et al. 2009). The ladder-like structure is widely accepted in the literature for pol para-PDA produced via chemical oxidation of monomer by sodium, potassium, or ammonium persulphate. The synthesized polymer shows high thermo stability and conductivity, high gas separation ability, and lyotropic liquid crystallinity (Chan et al. 1991; Cheng et al. 2006; Manivel et al. 2008; Prokeš et al. 1999; Sulimenko et al. 2001; Ullah et al. 2013). Another derivative of poly aniline is PBz which has been synthesized through chemical and electrochemical manner (D'Eramo et al. 2000; do Nascimento et al. 2004; Naveen Kumar et al. 2001). The presence of azo and phenanzine-like segments of PBz were detected by resonance Raman analysis (do Nascimento et al. 2004). However, some doubts concerning the structure of the polymer still remains. While FTIR, UV–Vis and ^{1}HNMR spectroscopies are commonly used in the study of aromatic diamine polymers, but there is not a real conclusion about the structure of these polymers in the literatures.

In the present work aniline, para phenylenediamine and benzidine polymers were synthesized via chemical and electrochemical oxidation. Then electrical and optical properties of the synthesized polymers were studied by cyclic potential sweep, IR and UV–Vis spectroscopic techniques. Some fundamental physical parameters such as energy levels and bandgaps were assessed for the polymer both theoretically and experimentally. Finally, by comparing the experimental and theoretical results the most probable structure for each polymer is predicted. This study reveals that the polymer structure strongly depends on the synthesis procedure.

Methodology

Experimental

Materials

Aniline, para phenylenediamine and benzidine (reagent grad) were purchased from Merck. Aniline was distilled under reduced pressure and kept far from the light in the refrigerator for subsequent uses. Other chemicals (reagent grade) were purchased from Merck and used without further purification. Conductive glass (FTO glass, sheet resistance 8 Ωsq^{-1} purchased from South Korea) was used as working electrode.

Methods

PANI, PpPDA, PBz were synthesized by a chemical and electrochemical oxidative polymerization method at ambient temperature. Ammonium peroxy disulphate (APS) and HCl were used as oxidizing agent and supporting electrolyte, respectively. In a typical procedure, 10 mL (0.1 M) of HCl were mixed with 1.14 g sodium dodecyl sulfate (SDS) and stirred. 10 mL (0.15 M) of each monomer (aniline, para phenylenediamine and benzidine) were added and stirred for one hour. Then 10 mL of APS (0.04 M) were also mixed. The reaction was continued for 5 h in stirred solution. The mixture was filtered and washed with distilled water, methanol and then with HCl (0.1 M).

The electrochemical method such as cyclic voltammetry (CV), is commonly used in studies of small molecules and polymers (Heinze 1984). Oxidation (π_{ox}) and reduction(π_{red}) potentials can be used for estimating the values of solid state ionization potentials(I), electron affinities and experimental band gap (Sworakowski 2018; Sworakowski and Janus 2017; Sworakowski et al. 2016). The electrochemical polymerizations were also performed in a single compartment cell housing three-electrodes at room temperature using cylic potential sweep ethodd. FTO was used as working and a Pt rod as counter electrodes, respectively. All reported potentials were measured relative to Ag/AgCl/Cl^{-}(sat.) reference electrode. The electrochemical polymerization was carried out in $NaClO_4$ solution containing 0.04 M monomer on FTO working electrodes. Polymers were deposited by potential cycling between − 0.3 and 1.4 V at scan rate of 50 mVs^{-1}. Experimental band gaps were calculated by the difference between HOMO and LUMO states which are the negative values of ionization potentials (I) and the electron affinities (A). Commonly used procedure (Cardona et al. 2011) (Eq. 1) were for calculating I and A values.

$$I = e\pi_{ox} + 4.8\ \text{eV}; \quad A = e\pi_{red} + 4.8\ \text{eV} \tag{1}$$

In the above equation, the parameter e stands for the unite charge. The energies are expressed in eV.

Electrochemical studies were carried out using an Autolab general purpose electrochemical potentiostat/galvanostat system PG302N.

Electronic absorption spectra were obtained on an Agilent UV–visible spectrometer (model 8453, USA). IR spectra

were recorded using a Shimadzu model 470 grating IR measurement instrument by the KBr pellet technique.

Computational methods

DFT and time dependent DFT calculations (TDDFT) were performed to determine the approximate structure of poly aniline, poly para phenylenediamine and polybenzidine. It was shown that oligomers up to five or six repeating units can accurately represent the polymeric properties (Kamran et al. 2015; Ullah et al. 2014). Different types of geometries were considered for these polymers that are presented in Figs. 1, 8 and 18. All structures were optimized using B3LYP/6-31G(d) method which was proposed to give fruitful results especially in the field of conducting polymers (Kamran et al. 2015; Salzner 2008; Ullah et al. 2013; Ullah et al. 2014; Yang et al. 2006). HOMO-LUMO energy gaps and IR spectra of all oligomers were simulated using the same method and scaled with a scaling factor of 0.9631 (Casado et al. 1999; Kamran et al. 2015). The UV–Vis spectra and optical energy gaps were simulated at TD-DFT/6-31G(d) level of theory using polarized continuum solvation model (PCM) in dimethylsulfoxide medium (Tomasi et al. 2005). All calculations were performed with GAUSSIAN 09 (Frisch et al. 2009) program and visualization of results were done with Gauss View 5 visualization software (Dennington et al. 2009).

Results and discussion

Poly aniline

Structural and electronic properties

Figure 1 shows two oxidation states of poly aniline that may be obtained through our synthesized procedure which are called *PAni-a* and *PAni-b* for leucoemeraldine and emeraldine structures, respectively. The optimized geometry structures are presented in Fig. 2 showing that both structures are twisted to minimize steric hindrance of hydrogen atoms. Table 1 shows the inter ring bond lengths and torsional angles. This non planar structure reduces the delocalization

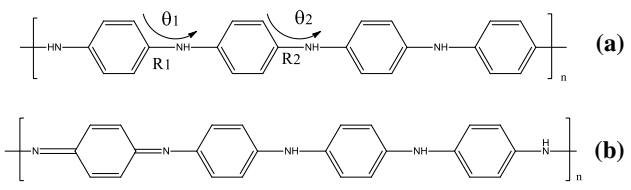

Fig. 1 Proposed structures of aniline **a** Leucoemeraldine (*PAni-a*), **b** Emeraldine (*PAni-b*)

of π- electrons along the polymer backbone leading to reduction of polymer conductivity. The C-N bond lengths and torsional angles in *PAni-a* structure were calculated to be about 1.40 Å and 35-40º, respectively.

In *PAni-b* structure, torsional angles around C=N bonds are lower than those of calculated for *PAni-a*. The lower torsion increases the electron delocalization and reduces the bond length in *PAni-b* chain. The HOMO–LUMO delocalization of both structures are presented in Fig. 2. It can be seen that HOMO is mostly distributed through C=C bonds of benzene and N atoms of polymers. However, in *PAni-b* it is distributed over C=N inter ring bonds and helps the electron delocalization. LUMO is located on C-N and C-H bonds of *PAni-a* with antibonding character. The LUMO state of *PAni-b* is mostly located on C atoms of benzene rings. However the band gap which was calculated by the difference between HOMO and LUMO levels is about 3.93 eV and 2.16 eV in *PAni-a* and *PAni-b* chains, respectively.

Figure 3 shows the CV for electrochemically synthesized PANI obtained in CH_3CN solution containing 0.1 M $NaClO_4$ by scan rate of 50 mV/s. Oxidation and reduction potentials are presented in Table 2. The anodic peak relevant to the oxidation of poly aniline is observed at 1.48 V and its cathodic peak is appeared at -1.41 V. Using Eq. 1 gives the band gap of 2.89 eV which is close to the band gap of *PAni-b* structure. In order to clear the ambiguity in the determination of the band gap and the structure of the polymers spectroscopic techniques were considered.

UV–Vis characterization of polymers

The experimental UV–Vis spectrum of aniline dissolved in DMSO is shown in Fig. 4a and the simulated one is depicted in Fig. 5. The experimental UV–Vis spectrum shows distinctive absorption peaks at 330, 390 and 540 nm. The peak appeared at 330 nm corresponds to π-π^* excitation of para substituted benzoid segment in PANI which is in close agreement with the peaks appeared at 320 and 354 nm for *PAni-a* and *PAni-b* structures, respectively (Nateghi and Savabieh 2014; Shahhosseini et al. 2016). The peak observed at 390–460 nm region in experimental spectrum is attributed to polaronic transitions of quinoidal structure which can be correlated to the peak presents at 480–500 nm in simulated spectrum of *PAni-b* structure.

The broad peak observed at 500–800 nm in experimental spectrum shows nice correlation with the low intensity peak appeared in *PAni-b* spectrum. On the basis of this similar assignments and band peak position it can be concluded that the PANI structure of synthesized sample is *PAni-b*. Simulated optical band gaps (ΔE_g^{opt}) of two structures are presented in Table 2.

The optical band gap of synthesized structure can be determined by calculating the electron transitions between

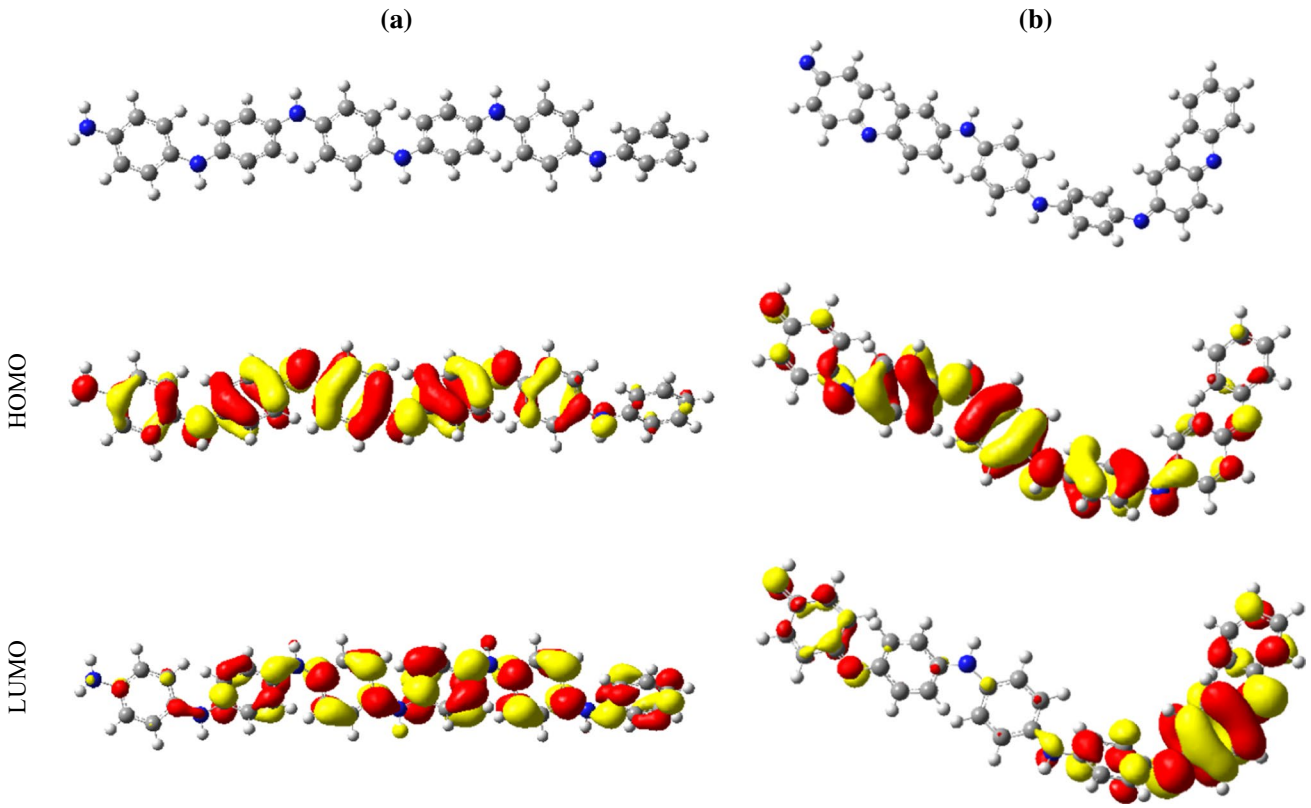

Fig. 2 Optimized structures and frontier orbitals at isovalue = 0.02 of **a** Leucoemeraldine (PAni-a), **b** Emeraldin (PAni-b)

Table 1 Torsional angles (°) and bond lengths (Å) of Ani-a and Ani-b. The parameters are shown in studied structure figures

Θ_2 (°)	Θ_3 (°)	Θ_4 (°)	Θ_5 (°)	R_1 (Å)	R_2 (Å)	R_3 (Å)	R_4 (Å)	R_5 (Å)
36.28	−32.26	30.81	38.36	1.40	1.40	1.40	1.40	1.40
−20.90	−30.74	38.16	−10.88	1.39	1.39	1.40	1.39	1.30

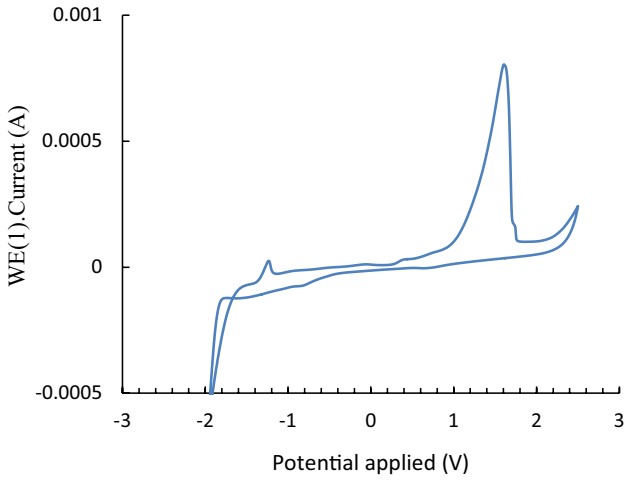

Fig. 3 Cyclic votammogram of PANI coated FTO electrode immersed in 0.1 M $NaClO_4$ in CH_3CN. sweep rate; 50 mVs^{-1}

Table 2 The experimental and calculated HOMO–LUMO energies with electronic (ΔE_g^{H-L}) and optical (ΔE_g^{opt}) band gaps of all proposed structures of PANI

Structure	HOMO/eV	LUMO/eV	ΔE_g^{H-L} (eV)	ΔE_g^{opt} (eV)
Ani-a	−4.083	−0.1573	3.93	3.37
Ani-b	−4.825	−2.6665	2.16	1.71
Ani-exp	−6.28	−3.39	2.89	1.90

the highest occupied valence band and the lowest unoccupied conduction band started at the absorption edge of the absorption spectrum. The optical band gap energy is obtained by Tauc's equation (Bhatt et al. 2012):

$$\alpha h\nu = A\left(h\nu - \Delta E_g\right)^n \quad (2)$$

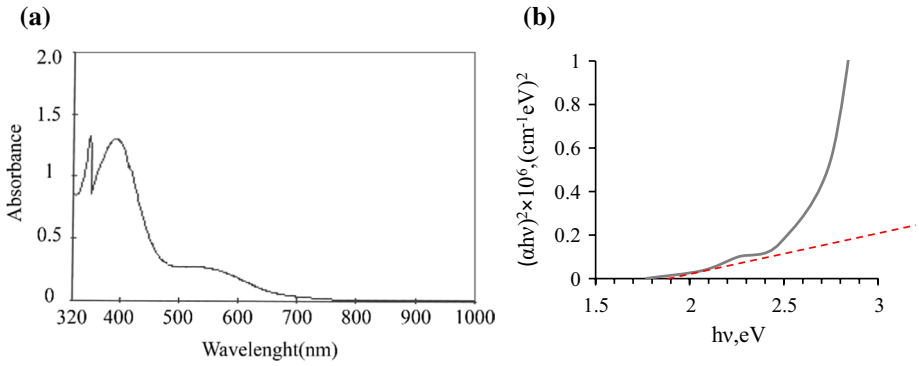

Fig. 4 **a** UV–Vis spectrum, **b** Tauc's plot from UV–visible analysis of poly aniline dissolved in DMSO

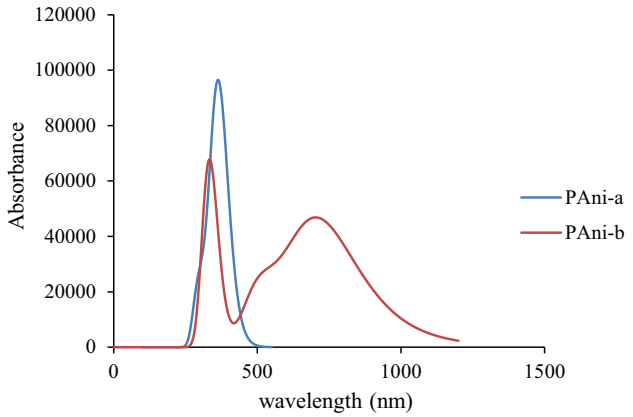

Fig. 5 Simulated UV–Vis spectra of aniline **a** Leucoemeraldine (*PAni-a*), **b** Emeraldin (*PAni-b*)

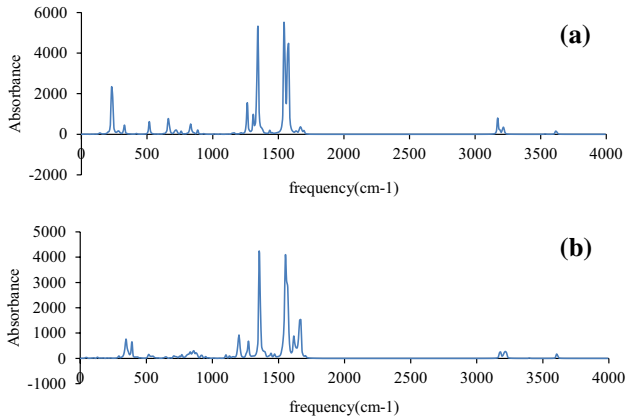

Fig. 6 Theoretical IR spectra of aniline **a** Leucoemeraldine (*Ani-a*), **b** Emeraldin (*Ani-b*)

where $h\nu$ is the photon energy, h is Planck's constant, α is the absorption coefficient, ΔE_g is the optical energy gap, A is a constant, and n is an index which shows the characteristics of electron transition in a semiconductor, i.e., $n = 1/2$ for allowed direct transition and $n = 2$ for allowed indirect band transition (Davis and Mott 1970; Shahhosseini et al. 2016). The optical band gap is calculated by this equation and $(\alpha h\nu)^2$ vs. $h\nu$ was plotted and the extrapolated to $(\alpha h\nu)^2 = 0$ (Fig. 4b). ΔE_g was obtained to be 1.90 eV for poly aniline which is in good correlation with theoretical one calculated for *PAni-b* structure (1.71 eV). However, *PAni-a* gives the band gap of 3.37 eV. Therefore, it can be concluded that poly aniline is synthesized with the structure labeled as *PAni-b* (Fig. 1b).

Vibrational spectral characteristics of poly aniline

Calculated IR spectra of proposed structures of poly aniline and corresponding experimental spectra are presented in Figs. 6 and 7, respectively. Comparisons between observed and simulated bands are listed in Table 3. The experimental N–H stretching band is appeared at about 3580 cm^{-1} while the simulated bands are computed to be at about 3477 and 3467 cm^{-1} in *PAni-a* and *PAni-b* structures, respectively. The discrepancies from experimental data are due to the fact that the theoretical data are obtained for an isolated oligomer in the vacuum state whereas the experimental one is achieved in condensed phase. The band observed at about 3230 cm^{-1} in experimental spectrum is attributed to C–H stretching vibrations of aromatic rings. The corresponding bands in simulated spectra can be observed at about 3100 and 3106 cm^{-1} in *PAni-a* and *PAni-b*, respectively.

The appearance of distinct band relevant to C=N vibration at 1567 cm^{-1} which is clearly observable in IR spectrum of *PAni-b* is a very good evidence of formation of *PAni-b* structure. In corresponding simulated spectrum, C=N vibration is appeared at 1517 cm^{-1}. Moreover, presence of a broad peak at 853 cm^{-1} which is relevant to C-H out of plane vibration is another proof to adopt the *PAni-b* as the structure of synthesized poly aniline.

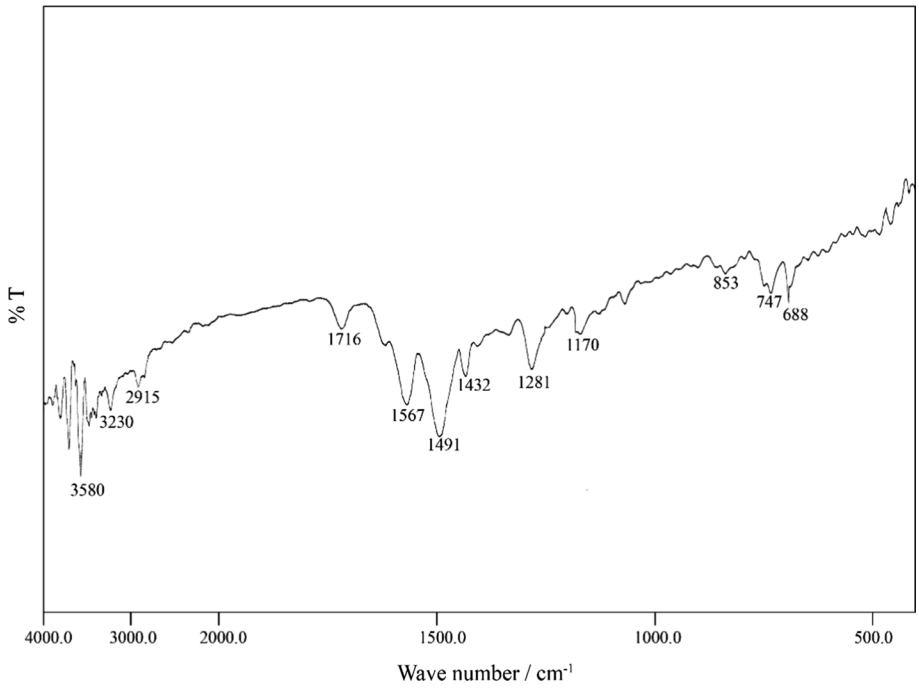

Fig. 7 Experimental IR spectrum of poly aniline in KBr pellet

Table 3 Experimental and calculated frequencies (cm^{-1}) of poly aniline

	Exp	Type a	Type b	Approximate assignment
1	3805	3477	3467	N–H stretching
2	3230	3100	3106	C–H stretching
3	1716	1630	1639	C=C stretching
4	1567	–	1517	C=N stertching
5	1491	1463	1479	N–H wag
6	1281	1298	1325	C–N, C-Hwag
7	1170	1210	1159	C–H sic
8	853	806.5	813	C–H wag

Poly para phenylenediamine

Structural and electronic properties

The proposed and optimized structures for poly para phenylendiamines are depicted in Fig. 8, 9, 10, 11, 12, respectively. Inter ring bonds and angles are presented in Table 4. It can be seen that the structures are twisted to minimize steric hindrance. The bridging angles are about 150° in *PPDA-a* structure with a bond length of 1.41 Å. The high conjugated *PPDA-b* structure is planar and the bond lengths are about 1.31–1.36 Å. *PPDA-c* structure is also

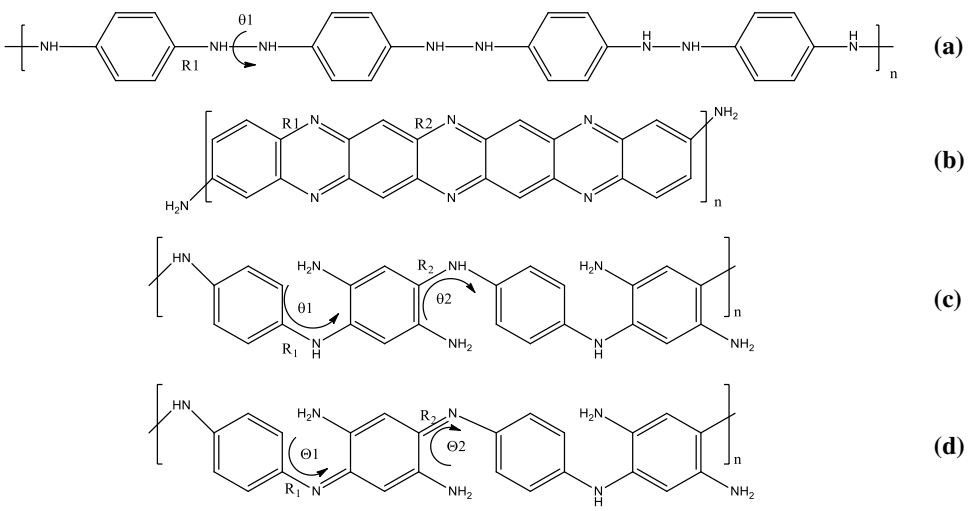

Fig. 8 Proposed structures of poly para phenylenediamine **a** PPDA-a, **b** PPDA-b, **c** PPDA-c, **d** PPDA-d

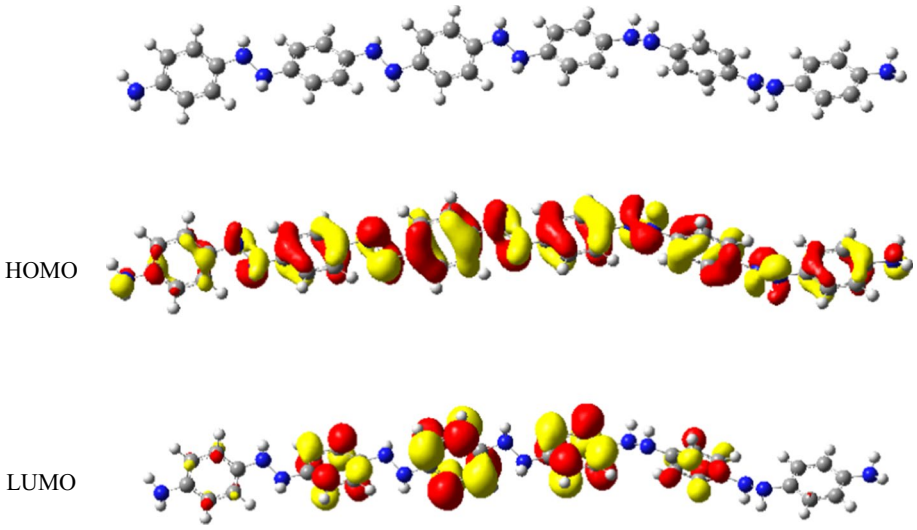

Fig. 9 Optimized structures and frontier orbitals at isovalue = 0.02 of PPDA-a structure of PpPDA

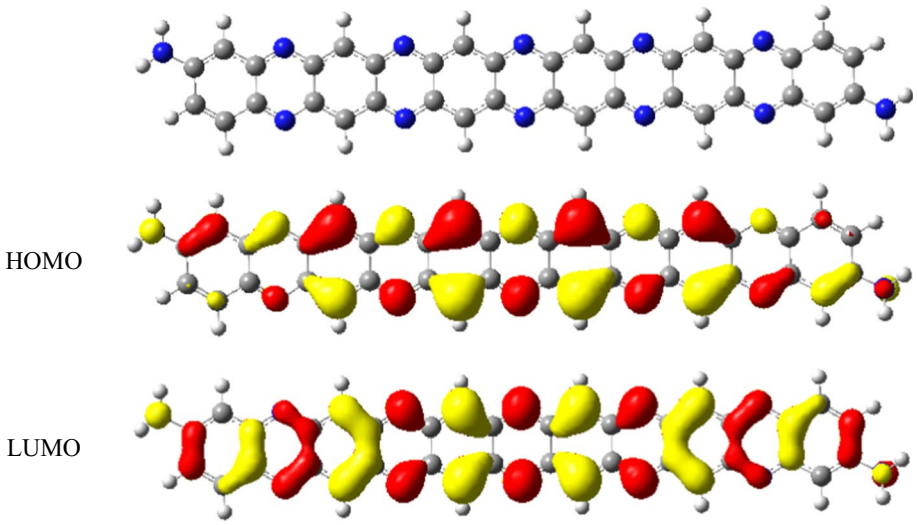

Fig. 10 Optimized structures and frontier orbitals at isovalue = 0.02 of PPDA-b structure of PpPDA

Table 4 Torsional angles (°) and bond lengths (Å) of proposed PpPDA structures. The parameters are shown in studied structure figures

	Θ_1 (°)	Θ_2 (°)	Θ_3 (°)	Θ_4 (°)	Θ_5 (°)	R_1 (Å)	R_2 (Å)	R_3 (Å)	R_4 (Å)	R_5 (Å)
PPDA-a	150.0	−148.5	150.5	148.3	−150.2	1.42	1.41	1.41	1.41	1.41
PPDA-b	−0.143	0.0076	0.0024	0.0050	0.099	1.31	1.33	1.34	1.35	1.36
PPDA-c	−48.33	15.06	44.89	17.96	46.51	1.41	1.41	1.40	1.41	1.40
PPDA-d	−43.60	9.865	37.64	19.53	44.84	1.40	1.31	1.40	1.41	1.40

twisted to reduce the steric hindrance of amine groups. The bridging angles are alternating between 48° and 15° and the bond lengths are about 1.41 Å in this structure.

The structure is twisted the most in *PPDA-d*. Bridging angles are about 44° around single C–N bonds and it decreases to 10° around C=N bonds. The bond lengths are alternating between 1.31 Å and 1.40 Å for double and single C–N bonds, respectively.

The twisted structure in *PPDA-d* leads to the separation of HOMO–LUMO states and the conductivity reduction. The HOMO–LUMO distributions of all structures are depicted in Figs. 9, 10, 11, 12. The results show that in *PPDA-a*, the HOMO is mostly distributed over the benzene rings and N–N bonds with bonding property whereas the LUMO is located on C atoms of benzene rings. This distribution leads to the band gap of 4.69 eV in this structure. In

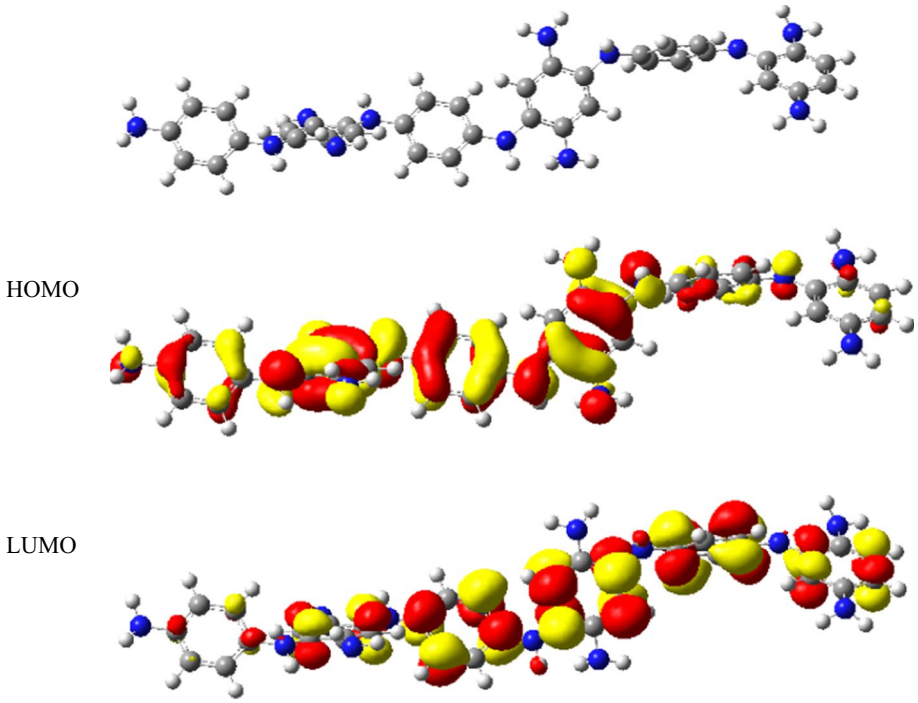

Fig. 11 Optimized structures and frontier orbitals at isovalue = 0.02 of PPDA-c structure of PpPDA

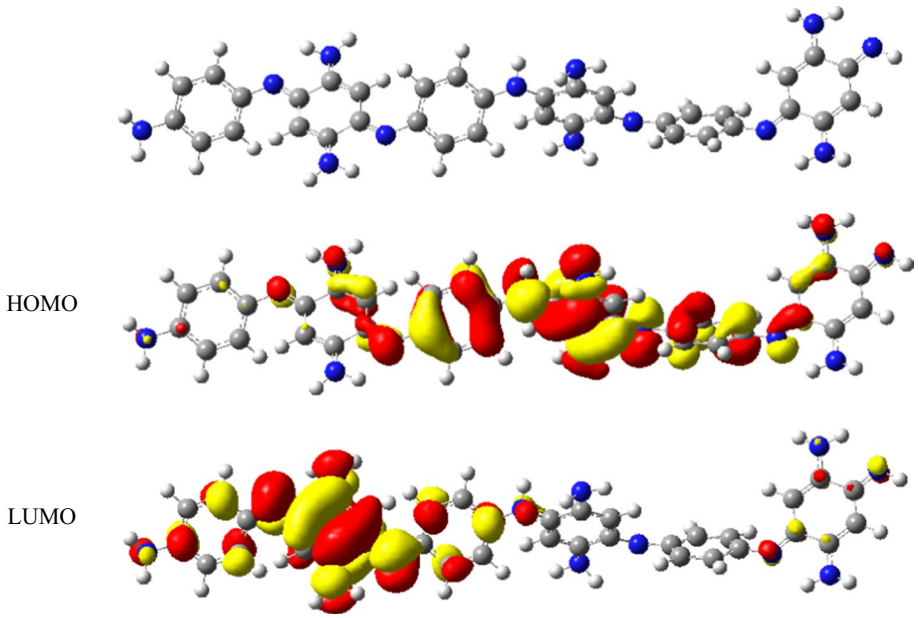

Fig. 12 Optimized structures and frontier orbitals at isovalue = 0.02 of PPDA-d structure of PpPDA

PPDA-b, HOMO–LUMO states that are distributing on C=C and C=N bonds overlap, leading to easier electron transfer in this structure. Therefore the band gap reduces to 0.91 eV in agreement with previous calculations (Yang et al. 2014).

In *PPDA-c* structure, HOMO is mostly distributed over C=C of benzene rings and C–N inter ring bonds. LUMO is mostly located over C atoms of aniline rings and some C–N bonds which are overlapping with HOMO. The calculated band gap for this structure is 3.93 eV. HOMO state of *PPDA-d* is mostly distributed over the C=C and C=N bonds which overlaps with LUMO state and is distributed over C–N bonds and resulting delocalization of electrons through the polymer backbone. The HOMO–LUMO gap which is theoretically obtained for this structure is 2.27 eV. The experimental band gaps obtained electrochemically are presented in Table 5. The cyclic voltammogram in Fig. 13 shows that PpPDA is electroactive and the peaks occurring at the potentials $\pi_{ox} = 1.60$ and $\pi_{red} = -1.35$ V correspond to the oxidation and reduction of the polymer, respectively.

Table 5 The experimental and calculated HOMO–LUMO energies with electronic (ΔE_g^{H-L}) and optical (ΔE_g^{opt}) band gaps of proposed structures of PpPDA

Structure	HOMO/eV	LUMO/eV	ΔE_g^{H-L} (eV)	ΔE_g^{opt} (eV)
PPDA-a	−4.50	0.195	4.69	4.09
PPDA-b	−4.91	−4.00	0.91	0.62
PPDA-c	−3.94	−0.0161	3.93	3.37
PPDA-d	−4.24	−1.97	2.27	1.86
PPDA-exp	−6.40	−3.45	2.95	2.48

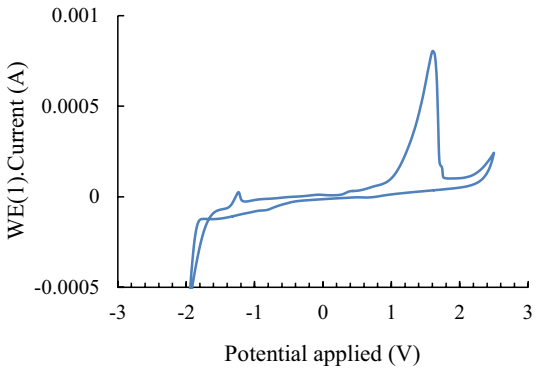

Fig. 13 Cyclic votammogram of PpPDA coated FTO electrode immersed in 0.1 M $NaClO_4$ in CH_3CN. sweep rate; 50 mVs^{-1}

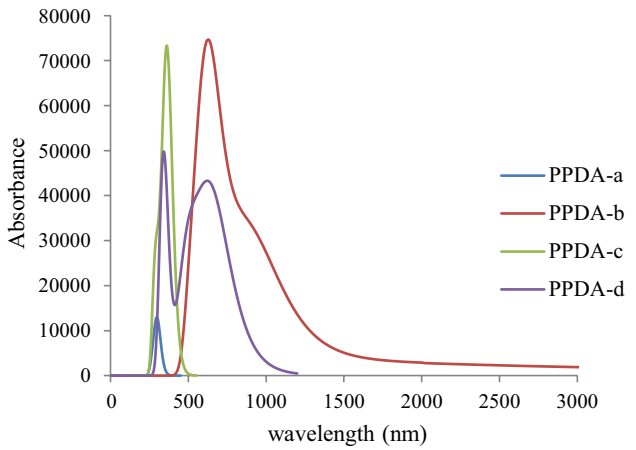

Fig. 14 simulated UV–Vis spectra of poly para phenylenediamine **a** PPDA-a, **b** PPDA-b, **c** PPDA-c, **d** PPDA-d

The results show that the experimental band gap obtained using Eq. 1 is close to that of *PPDA-d* structure. Therefore, in order to determine the most probable structure in accordance with the obtained results, it is necessary to investigate the optical properties of the proposed structures.

UV–Vis spectra characterization

Simulated UV–visible spectra of all structures are depicted in Fig. 14. It can be seen that, among proposed structures, *PPDA-a* has the lowest absorption coefficient. The absorption peak appeared at short wavelengths ($\lambda_{max} = 303$ nm) indicates low conjugation compared to other structures. On the other hand the highest absorption coefficient and λ_{max} are related to the *PPDA-b* structure since of its highly conjugated form. The peaks related to π–π^* electron transitions are appeared at 859 and 592 nm. *PPDA-c* shows two peaks that are appeared at 368 and 283 nm.

Figure 15 shows the experimental spectrum of PpPDA. Two peaks that are appeared in 345 and 667 cm^{-1} show nice correlation with *PPDA-d* structure. The optical band gap calculated using DFT calculations is 1.86 eV for *PPDA-d* structure and that one obtained by Tauc's plot (Eq. 2) is 2.48 eV (Fig. 15b) which is in more agreement with that obtained for the *PPDA-d* structure (Table 5). The discrepancy between experimental and theoretical data can be attributed to the limited length of oligomer and the approximation that was taken into account for solvation model in simulated spectrum.

Vibrational spectral characteristics of poly para phenylendiamines

Calculated IR spectra of all structures are shown in Fig. 16 and the experimental one is depicted in Fig. 17. Table 6 shows the experimental and calculated vibration frequencies of PpPDA. N–H stretching band is appeared at about 3303 cm^{-1} in *PPDA-a* spectrum. However it is observed at 3406 cm^{-1} in *PPDA-c* and *PPDA-d* spectra. Since there are two different types of N–H bonds (NH and NH_2) in two last structures, the broad band at 3210–3365 cm^{-1} of experimental spectrum confirm that synthesized form of PpPDA corresponds to *PPDA-c* or *PPDA-d* structures. NH_2 bending is observed at 1631 and 1626 cm^{-1} in *PPDA-a* and *PPDA-b* spectra, respectively. The corresponding band in experimental spectrum is appeared at about 1634 cm^{-1}.

A high intensity band that is observed at 1514 cm^{-1} in experimental spectrum can be attributed to C=C and C=N stretching in all proposed structures. However, C=N stretching of *PPDA-b* is observed at 1442 cm^{-1} and that of *PPDA-d* is appeared at 1520 cm^{-1} which is in very good accordance with experimental one. N–N stretching in PPDA-a structure is appeared at 1128 cm^{-1} with high intensity which is not observed in experimental spectrum. Therefore, *PPDA-a* cannot be the right structure of synthesized PpPDA. Also the calculated C–N stretching band for *PPDA-d* (1238 cm^{-1}) is nearly same as experimental one (1232 cm^{-1}) indicating that the *PPDA-d* structure is the most probable to consider for PpPDA.

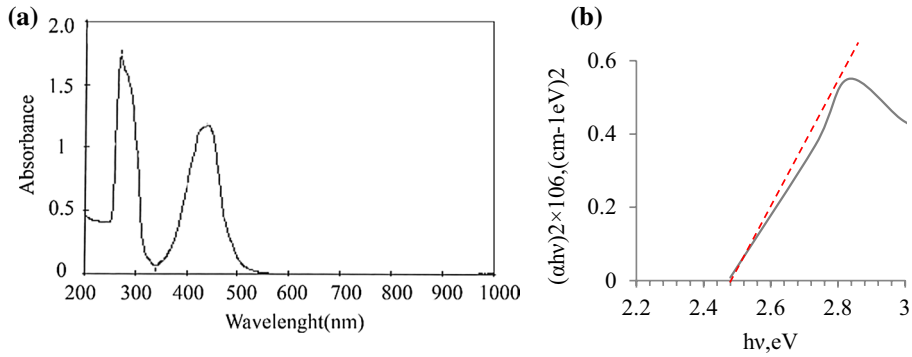

Fig. 15 **a** UV–Vis spectrum, **b** Tauc's plot from UV–visible analysis of PpPDA dissolved in DMSO

Poly benzidine

Structural and electronic properties

Different proposed structures of poly benzidine (PBz) are shown in Fig. 18. All hexamer structures were optimized and are presented in Figs. 19, 20, 21. Figure 19 shows that *PBz-a* is twisted more than other structures which resulted in the lowest conjugation of the structure. The structural parameters presented in Table 7 show that the dihedral angles about NH bridge are about 143–145°. However, the torsional angles between two benzene rings are about 36°.

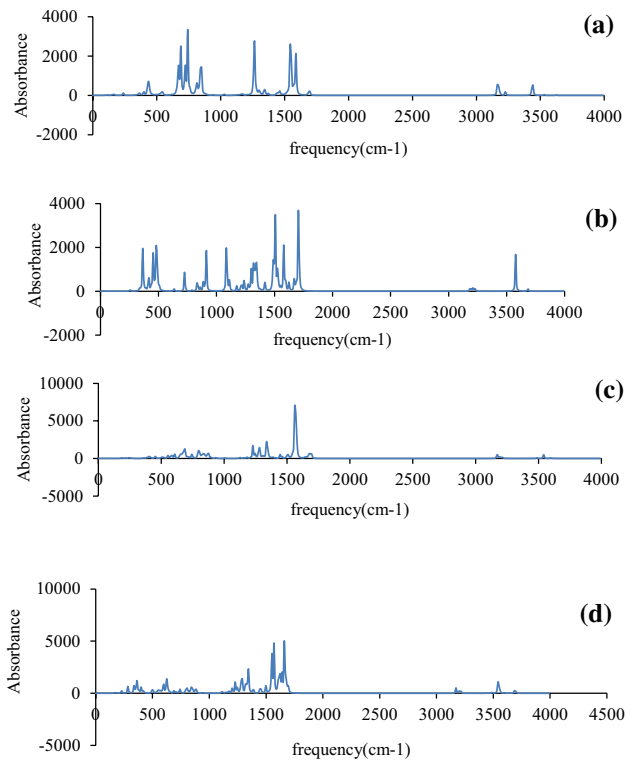

Fig. 16 Scaled IR spectra of poly para phenylenediamine **a** PPDA-a, **b** PPDA-b, **c** PPDA-c, **d** PPDA-d

This twisted structure with long bond lengths limits the electron conjugations and increases the band gap.

The dihedral angles on N–N bridges of *PBz-b* are about 180°. The dihedral angles between two benzene rings with single and double bonds are about 33° and 2–5°, respectively. The N–N and C–N bond lengths are about 1.33 Å and the inter ring bond lengths vary between 1.48 and 1.41 Å for single and double bonds, respectively. These structures compared to, show more electron mobility through the polymer backbone and reduced band gap compared to *PBz-a*. In *PBz-c*, the C–C bonds are twisted about 33°. The C–C bond lengths are about 1.48 Å.

HOMO–LUMO distributions of proposed structures are also shown in Figs. 16, 17, 18. It can be seen that HOMO states of *PBz-a* are mostly distributed over the benzene rings and N–N inter ring bonds. LUMO states are located on C–C inter ring bonds and C atoms of benzene segment. This distribution leads to the energy gap of 4.53 eV. However, HOMO is delocalized over the C=C and C=N bonds of *PBz-b*. The LUMO states are also distributed over the next part of the chain and help the electron transfer through the polymeric chain. Consequently, the band gap reduces to 1.23 eV. The twisted structure in *PBz-c* decreases the HOMO delocalization over the chain. However, they are distributed over the benzene rigs and C-N bond. LUMO states are distributed over the rings and N atoms. They overlap with HOMO states to help the electron transfer through the chain. The band gap in this structure is 2.55 eV.

Cyclic voltammetry technique was used to find the experimental HOMO–LUMO gap of synthesized polybenzidine. The PBz voltammogram presented in Fig. 22 shows an anodic peak at 1.58 V and a broad reduction peak centered at about − 1.35 V. The HOMO–LUMO gaps calculated using Eq. 1 are depicted in Table 8.

UV–Vis spectra characterization

Simulated UV–visible spectra of all proposed structures are presented in Fig. 23. A sharp peak at 310 nm is observed

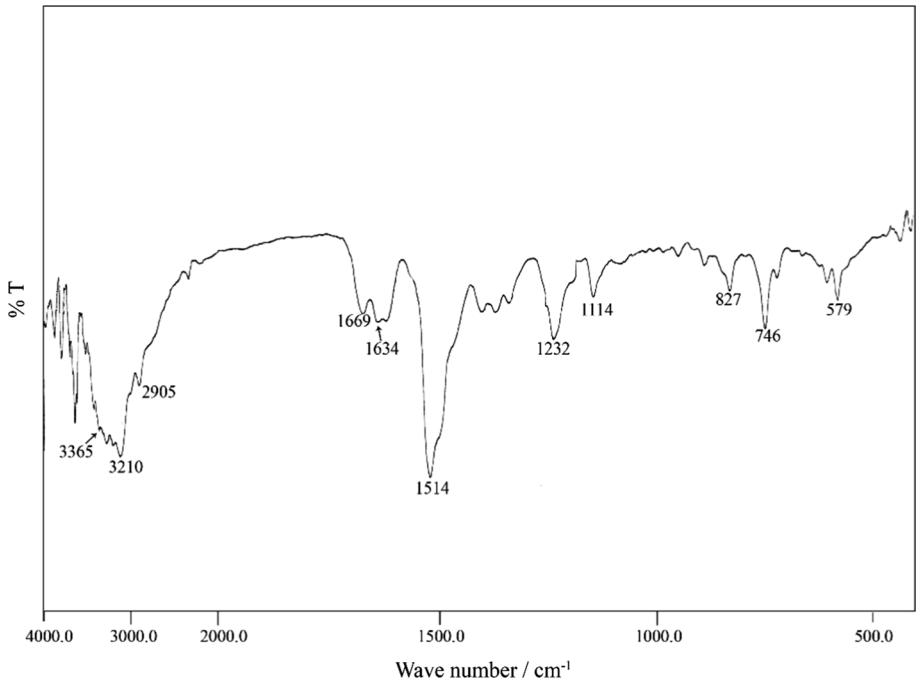

Fig. 17 Experimental IR spectrum of PpPDA in KBr pellet

Table 6 Experimental and calculated frequencies (in cm^{-1}) of PpPDA

	IR/Exp	Type a	Type b	Type c	Type d	Approximate assignment
1	3365	3303	–	3406	3409	N–H stretching
2	2905	3046	3110	3080	3070	C–H stretching
3	1634	–	–	1631	1629	NH_2 bending
	1514	1586	1588	1551	1581	C=C stretching
4	1514	–	1442	–	1520	C=N stertching
	–	1128	–	–	–	N–N stretching
5	1232	1222	1045	1249	1238	C–N stretching
6	746	–	–	660	746	NH_2 wagging

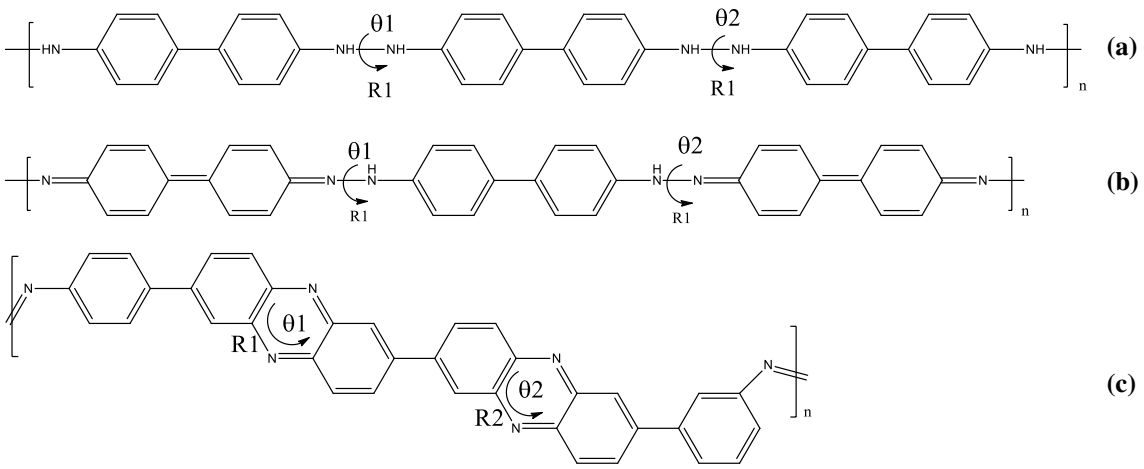

Fig. 18 proposed structures of poly benzidine **a** *PBz-a*, **b** *PBz-b*, **c** *PBz-c*

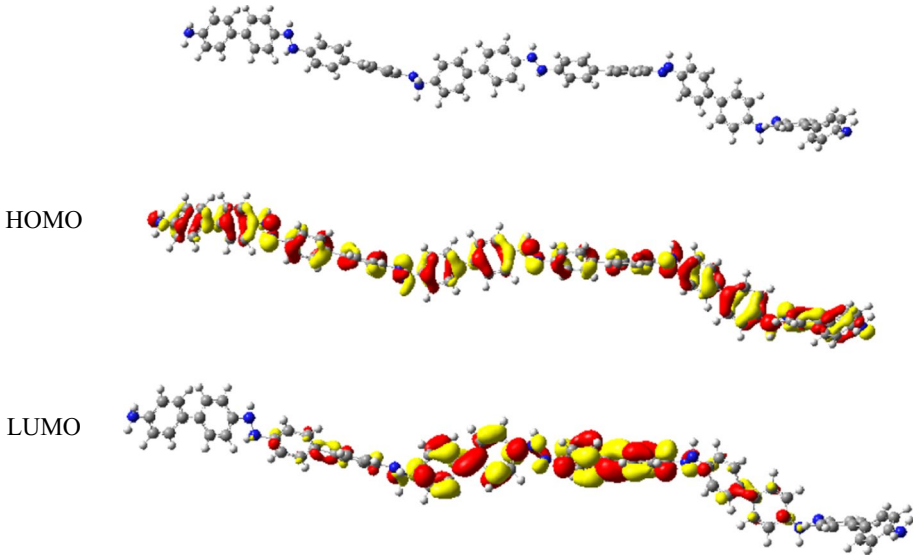

Fig. 19 Optimized structures and Frontier orbitals at isovalue = 0.02 of *PBz-a* structure of poly benzidine

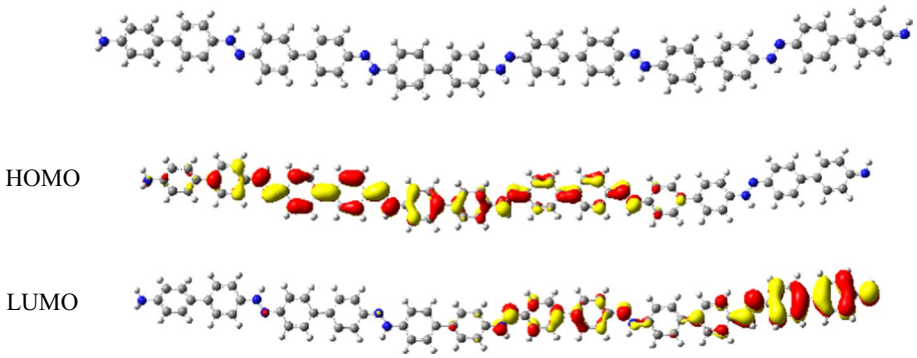

Fig. 20 Optimized structures and Frontier orbitals at isovalue = 0.02 of *PBz-b* structure of poly benzidine

for *PBz-a* structure. Higher conjugation in *PBz-b* shifts the π–π* peak to 746 nm.

The broad peak observed at 565 nm in *PBz-c* spectrum has the best correlation with experimental one (λ_{max} = 455 nm) (Fig. 24a). The experimental optical gap is obtained 2.25 eV using Tauc's equation (Fig. 24b). As can be observed from Table 8, this band gap has also the best correlation with *PBz-c* structure. Therefore, it can be concluded that the *PBz-c* is the most probable structure for synthesized PBZ.

Vibrational spectral characteristics of poly benzidine

Simulated IR spectra of three proposed structures and the experimental spectrum are presented in Figs. 25 and 26, respectively. Table 9 shows the calculated vibration frequencies of all structures. N–H stretching band is appeared at 3460 cm^{-1} in *PBz-a* structure. It is observed at 3264 cm^{-1} with lower intensity in *PBz-b* spectrum. The peaks for N–H in *PBz-c* are due to the ends of the oligomer. However, there is no distinguished peak for N–H in experimental spectrum which confirms the *PBz-c* structure. C=N stretching which is expected to be appeared in *PBz-b* and *PBz-c* spectra are located at 1519 and 1506 cm^{-1}, respectively. It is appeared at 1487 cm^{-1} in experimental spectrum. C-H stretching at 2845 cm^{-1} of experimental spectrum has the best correlation with *PBz-c* structure (3099 cm^{-1}). Therefore, vibrational results also confirm that the synthesis procedure leads to the ortho-coupling of benzidine and formation of phenazine segment *(PBz-c)* structure.

Table 10 shows a comparison between three aniline based structures. It can be seen that our synthesized procedure leads to the formation of benzoid form of PANI and PpPDA (PAni-b and PPDA-d) and phenazine form of PBZ (PBz-c). Experimental HOMO–LUMO gaps are ~ 2.9 eV in these structures which show that the electrochemical oxidative polymerization can affect the conductivity of synthesized polymers. The results also show that B3LYP calculations underestimate the HOMO–LUMO gap in all cases. Calculated ΔE_g^{H-L} of PANI is slightly smaller than those for other aniline based polymers. The results show that ΔE_g^{H-L} values are all greater than ΔE_g^{opt} values since it takes additional energy to fully separate electrons

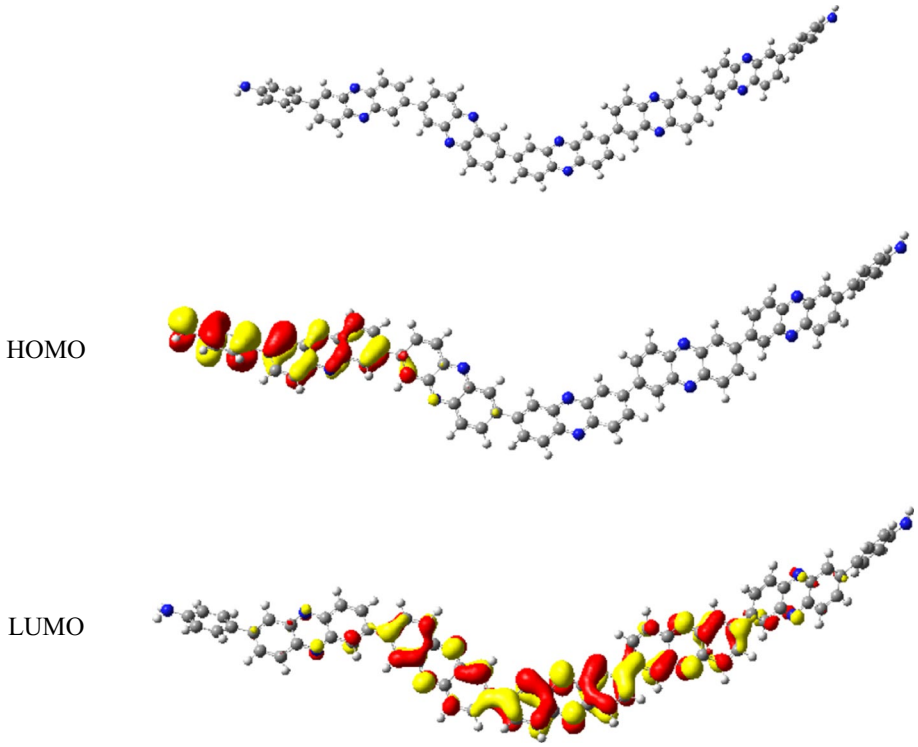

Fig. 21 Optimized structures and Frontier orbitals at isovalue = 0.02 of *PBz-c* structure of poly benzidine

Table 7 Torsional angles (°) and bond lengths (Å) of proposed PBz structures. The parameters are shown in studied structure figures

	Θ_1 (°)	Θ_2 (°)	Θ_3 (°)	Θ_4 (°)	Θ_5 (°)	R_1 (Å)	R_2 (Å)	R_3 (Å)	R_4 (Å)	R_5 (Å)
PBz-a	−143.5	146.3	143.1	144.4	144.4	1.40	1.40	1.39	1.39	1.39
PBz-b	−179.8	−180	−179.6	179.5	179.5	1.33	1.33	1.33	1.33	1.33
PBz-c	0.2799	0.3796	0.2344	0.2136	0.3040	1.33	1.34	1.34	1.34	1.35

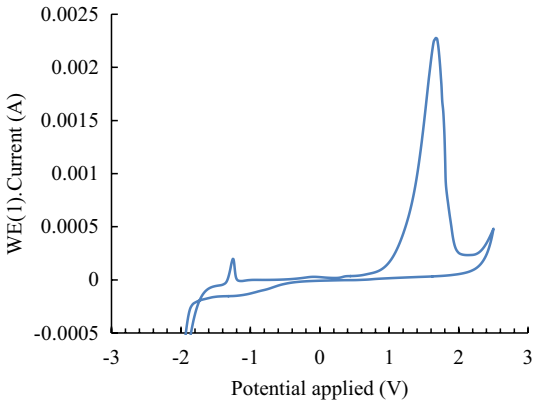

Fig. 22 Cyclic votammogram of PBz coated FTO electrode immersed in 0.1 M $NaClO_4$ in CH_3CN. sweep rate; 50 mVs^{-1}

and holes into free carriers (Franco Jr and Padama 2016). Obtained experimental results for optical band gaps show that PpPDA has the broadest band gap which leads to its lowest conductivity.

Table 8 The experimental and calculated HOMO–LUMO energies with electronic (ΔE_g^{H-L}) and optical (ΔE_g^{opt}) band gaps of all proposed structures of PBz

Structure	HOMO/eV	LUMO/eV	ΔE_g^{H-L} (eV)	ΔE_g^{opt} (eV)
PBz-a	−4.8	−0.2365	4.53	4.00
PBz-b	−4.082	−2.855	1.23	1.66
PBz-c	−5.378	−2.8267	2.55	2.19
PBz-exp	−6.38	−3.45	2.93	2.24

Conclusion

Various structures have been proposed for poly p-phenylene diamine in which monomers are linked via different reactive sites (ortho or para). Our combinatorial (theoretical and experimental) studies reveal that the ladder-type phenazine-like structure (PPDA-b) is the most probable among the proposed structures. Whereas, aniline monomers are linked together from para position to form polyaniline as emeraldine form. In the case of benzidine which

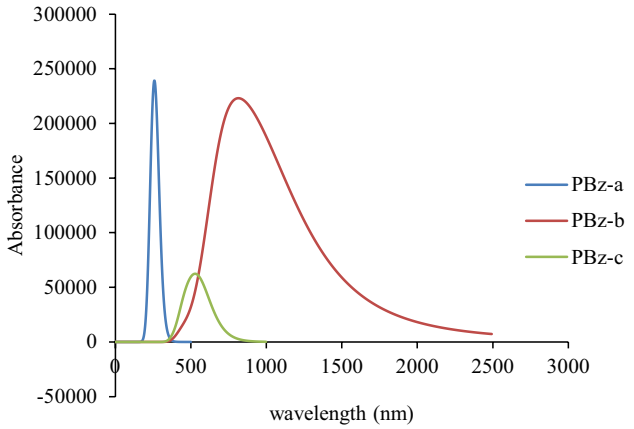

Fig. 23 Simulated UV–Vis spectra of poly benzidine a) *PBz-a,* b) *PBz-b,* c*) PBz-c*

is one of the dimers of aniline, most probable configuration is formed by binding the monomers via ortho and para positions, alternatively. Our results obtained from combinatorial studies indicated that for investigation of the complex structure of the conducting polymers it is necessary to hire various theoretical calculations and experimental techniques. Experimental band gaps were obtained through cyclic voltammetry and absorption spectroscopy and compared to HOMO–LUMO gaps from DFT calculations. Among the polymers investigated in this study the PANI shows lowest band gap (1.71 eV) which can be a good candidate for application as semiconductor in organic electronic.

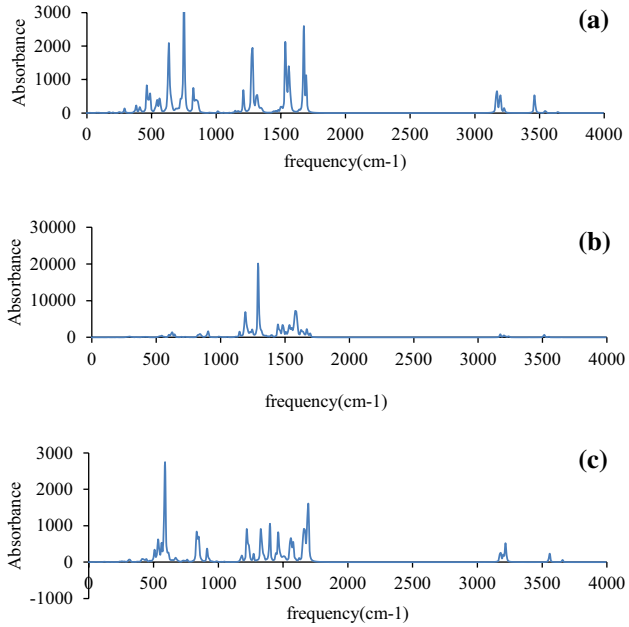

Fig. 25 Scaled simulated IR spectra of poly diphenylamine poly benzidine **a** PBz-a, **b** PBz-b, **c** PBz-c

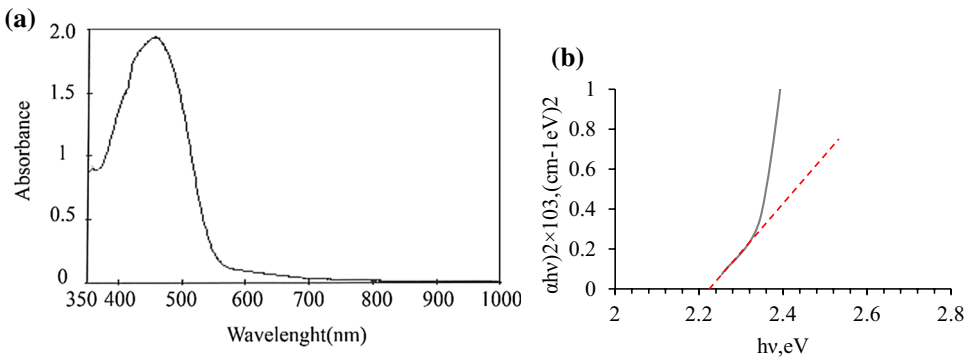

Fig. 24 **a** UV–Vis spectrum, **b** Tauc's plot from UV–visible analysis of poly benzidine dissolved in DMSO

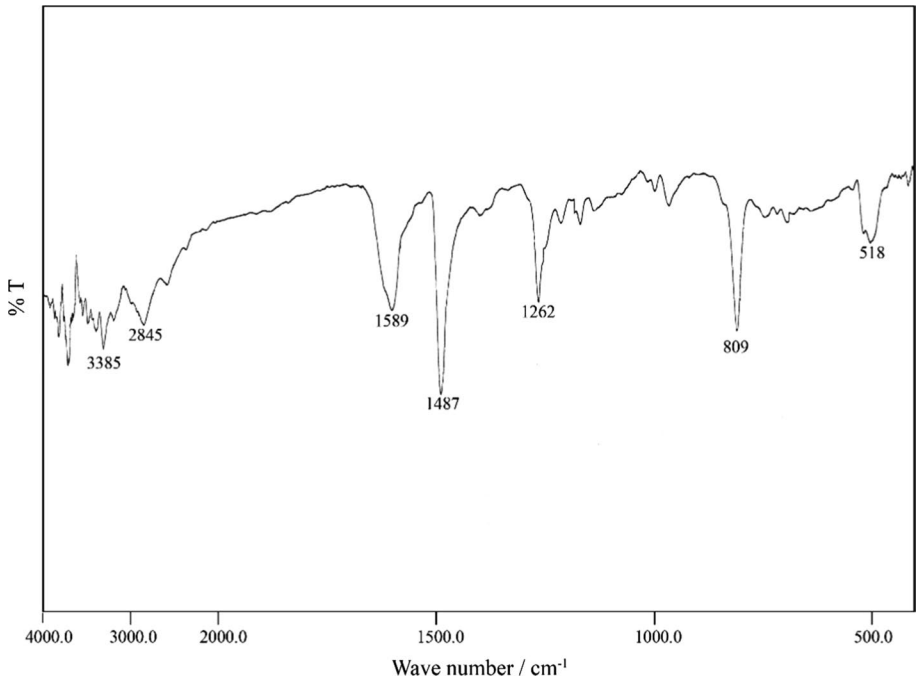

Fig. 26 Experimental IR spectrum of PBz in KBr pellet

Table 9 Experimental and calculated frequencies (in cm^{-1}) of PBz

	IR/Exp	Type a	Type b	Type c	Approximate assignment
1	–	3043	3046	–	N–H stretching
2	2845	3103	3118	3099	C–H stretching
3	1599	1605	1559	1589	C=C stretching
4	1487	–	1519	1506	C=N stertching
5	–	1087	1148	–	N–N stretching
6	809	816	823	800	C–N stretching
7	518	467	596	538	Ring- deformation

Table 10 The experimental and calculated electronic (ΔE_g^{H-L}) and optical (ΔE_g^{opt}) band gaps of all studied structures

Structure	ΔE_g^{H-L} (eV)(exp)	ΔE_g^{opt} (eV) (exp)	ΔE_g^{H-L} (eV)	ΔE_g^{opt} (eV)
PAni-b	2.89	1.90	2.16	1.71
PPDA-d	2.95	2.48	2.27	1.86
PB-z–c	2.93	2.24	2.55	2.19

References

Al-Hossainy AF, Zoromba MS (2019) Doped-poly (para-nitroaniline-co-aniline): synthesis, semiconductor characteristics, density, functional theory and photoelectric properties. J Alloy Compd 789:670–683. https://doi.org/10.1016/j.jallcom.2019.03.118

Al-Hossainy AF, Kh. Thabet H, Zoromba MS, Ibrahim A (2018) Facile synthesis and fabrication of a poly(ortho-anthranilic acid) emeraldine salt thin film for solar cell applications. New J Chem 42:10386–10395. https://doi.org/10.1039/C8NJ01204K

Amer I, Young DA (2013) Chemically oxidative polymerization of aromatic diamines: the first use of aluminium-triflate as a co-catalyst. Polymer 54:505–512. https://doi.org/10.1016/j.polymer.2012.11.078

Baibarac M, Baltog I, Smaranda I, Scocioreanu M, Lefrant S (2011) Hybrid organic–inorganic materials based on poly(o-phenylenediamine) and polyoxometallate functionalized carbon nanotubes. J Mol Struct 985:211–218. https://doi.org/10.1016/j.molstruc.2010.10.044

Bazito FFC, Silveira LT, Torresi RM, Córdoba-de-Torresi SI (2008) On the stabilization of conducting pernigraniline salt by the synthesis and oxidation of polyaniline in hydrophobic ionic liquids. Phys Chem Chem Phys 10:1457–1462. https://doi.org/10.1039/B714458J

Bhatt R, Bhaumik I, Ganesamoorthy S, Karnal AK, Swami MK, Patel HS, Gupta PK (2012) Urbach tail and bandgap analysis in near stoichiometric $LiNbO_3$ crystals. Phys Status Solidi A 209:176–180. https://doi.org/10.1002/pssa.201127361

Cardona CM, Li W, Kaifer AE, Stockdale D, Bazan GC (2011) Electrochemical considerations for determining absolute frontier orbital energy levels of conjugated polymers for solar cell applications. Adv Mater 23:2367–2371. https://doi.org/10.1002/adma.201004554

Casado J, Hernández V, Rami X, Rez FJ, López-Navarrete JT (1999) Ab initio HF and DFT calculations of geometric structures and vibrational spectra of electrically conducting doped oligothiophenes. J Mol Struct THEOCHEM 463:211–216. https://doi.org/10.1016/S0166-1280(98)00416-3

Chan HSO, Ng SC, Hor TSA, Sun J, Tan KL, Tan BTG (1991) Poly(m-phenylenediamine): Synthesis and characterization by X-ray photoelectron spectroscopy. Eur Polym J 27:1303–1308. https://doi.org/10.1016/0014-3057(91)90069-Z

Cheng F, Tang W, Li C, Chen J, Liu H, Shen P, Dou S (2006) Conducting poly(aniline) nanotubes and nanofibers: controlled synthesis and application in lithium/poly(aniline) rechargeable batteries. Chemistry 12:3082–3088. https://doi.org/10.1002/chem.200500883

Ćirić-Marjanović G (2013) Recent advances in polyaniline research: Polymerization mechanisms, structural aspects, properties and applications. Synth Met 177:1–47. https://doi.org/10.1016/j.synthmet.2013.06.004

Davis EA, Mott NF (1970) Conduction in non-crystalline systems V, Conductivity, optical absorption and photoconductivity in amorphous semiconductors. Philos Mag 22:0903–0922. https://doi.org/10.1080/14786437008221061

Dennington R, Keith T, Millam J (2009) GaussView, Version 5. Semichem Inc., Shawnee Mission

D'Eramo F, Silber JJ, Arévalo AH, Sereno LE (2000) Electrochemical detection of silver ions and the study of metal–polymer interactions on a polybenzidine film electrode. J Electroanal Chem 494:60–68. https://doi.org/10.1016/S0022-0728(00)00329-6

do Nascimento GM, Constantino VRL, Temperini MLA (2004) Spectroscopic characterization of doped poly(benzidine) and its nanocomposite with cationic clay. J Phys Chem B 108:5564–5571. https://doi.org/10.1021/jp037262i

Franco FC Jr, Padama AAB (2016) DFT and TD-DFT study on the structural and optoelectronic characteristics of chemically modified donor-acceptor conjugated oligomers for organic polymer solar cells. Polymer 97:55–62. https://doi.org/10.1016/j.polymer.2016.05.025

Frisch MJ et al (2009) Gaussian 09. Gaussian Inc, Wallingford

Guimard NK, Gomez N, Schmidt CE (2007) Conducting polymers in biomedical engineering. Prog Polym Sci 32:876–921. https://doi.org/10.1016/j.progpolymsci.2007.05.012

Heinze J (1984) Cyclic voltammetry—"electrochemical spectroscopy". New analytical methods (25). Angew Chem Int Edn Engl 23:831–847. https://doi.org/10.1002/anie.198408313

Kamran M, Ullah H, A-u-HA S, Bilal S, Tahir AA, Ayub K (2015) Combined experimental and theoretical study of poly(aniline-co-pyrrole) oligomer. Polymer 72:30–39. https://doi.org/10.1016/j.polymer.2015.07.003

Li X-G, Huang M-R, Duan W, Yang Y-L (2002) Novel multifunctional polymers from aromatic diamines by oxidative polymerizations. Chem Rev 102:2925–3030. https://doi.org/10.1021/cr010423z

Li T, Yuan C, Zhao Y, Chen Q, Wei M, Wang Y (2013) Facile Synthesis and characterization of poly (*o*-phenylenediamine) submicrospheres doped with glycine. J Macromol Sci Part A 50:330–333. https://doi.org/10.1080/10601325.2013.755882

Manivel P, Sathiyanarayanan S, Venkatachari G (2008) Synthesis of poly(p-phenylene diamine) and its corrosion inhibition effect on iron in 1M HCl. J Appl Polym Sci 110:2807–2814. https://doi.org/10.1002/app.28772

Min Y-L, Wang T, Zhang Y-G, Chen Y-C (2011) The synthesis of poly(*p*-phenylenediamine) microstructures without oxidant and their effective adsorption of lead ions. J Mater Chem 21:6683–6689. https://doi.org/10.1039/C1JM10169B

Muthirulan P, Rajendran N (2012) Poly(o-phenylenediamine) coatings on mild steel: electrosynthesis, characterization and its corrosion protection ability in acid medium. Surf Coat Technol 206:2072–2078. https://doi.org/10.1016/j.surfcoat.2011.09.008

Nateghi MR, Savabieh B (2014) Study of polyaniline oxidation kinetics and conformational relaxation in aqueous acidic solutions. Electrochim Acta 121:128–135. https://doi.org/10.1016/j.electacta.2013.12.111

Naveen Kumar M, Nagabhooshanam M, Anand Rao M, Bhagvanth Rao M (2001) Preparation and characterization of doped polybenzidine. Cryst Res Technol 36:309–317. https://doi.org/10.1002/1521-4079(200103)36:3<309:AID-CRAT309>3.0.CO;2-9

Prokeš J, Stejskal J, Křivka I, Tobolková E (1999) Aniline-phenylenediamine copolymers. Synth Metals 102:1205–1206. https://doi.org/10.1016/S0379-6779(98)01223-5

Salzner U (2008) Investigation of charge carriers in doped thiophene oligomers through theoretical modeling of their UV/Vis spectra. J Phys Chem A 112:5458–5466. https://doi.org/10.1021/jp800606m

Sapurina I, Stejskal J (2008) The mechanism of the oxidative polymerization of aniline and the formation of supramolecular polyaniline structures. Polym Int 57:1295–1325. https://doi.org/10.1002/pi.2476

Sayyah SM, El-Deeb MM, Kamal SM, Azooz RE (2009) Electropolymerization of o-phenylenediamine on Pt-electrode from aqueous acidic solution: Kinetic, mechanism, electrochemical studies and characterization of the polymer obtained. J Appl Polym Sci 112:3695–3706. https://doi.org/10.1002/app.29802

Sestrem RH, Ferreira DC, Landers R, Temperini MLA, do Nascimento GM (2009) Structure of chemically prepared poly-(para-phenylenediamine) investigated by spectroscopic techniques. Polymer 50:6043–6048. https://doi.org/10.1016/j.polymer.2009.10.028

Sestrem RH, Ferreira DC, Landers R, Temperini MLA (2010) Synthesis and spectroscopic characterization of polymer and oligomers of ortho-phenylenediamine. Eur Polym J 46:484–493. https://doi.org/10.1016/j.eurpolymj.2009.12.007

Shahhosseini L, Nateghi MR, Sheikh-Sivandi S (2016) Electrochemical synthesis of polymer based on 4-(2-thienyl)benzenamine in aqueous solutions: electrochemical properties, characterization and application. Synth Met 211:66–74. https://doi.org/10.1016/j.synthmet.2015.11.015

Stejskal J (2015) Polymers of phenylenediamines. Prog Polym Sci 41:1–31. https://doi.org/10.1016/j.progpolymsci.2014.10.007

Stejskal J, Gilbert RG (2002) Polyaniline. Preparation of a conducting polymer(IUPAC Technical Report). Pure Appl Chem 74:857–867. https://doi.org/10.1351/pac200274050857

Stejskal J, Kratochvíl P, Jenkins AD (1996) The formation of polyaniline and the nature of its structures. Polymer 37:367–369. https://doi.org/10.1016/0032-3861(96)81113-X

Stejskal J, Sapurina I, Trchová M (2010) Polyaniline nanostructures and the role of aniline oligomers in their formation. Prog Polym Sci 35:1420–1481. https://doi.org/10.1016/j.progpolymsci.2010.07.006

Sulimenko T, Stejskal J, Prokeš J (2001) Poly(phenylenediamine) Dispersions. J Colloid Interface Sci 236:328–334. https://doi.org/10.1006/jcis.2000.7415

Sworakowski J (2018) How accurate are energies of HOMO and LUMO levels in small-molecule organic semiconductors determined from cyclic voltammetry or optical spectroscopy? Synth Met 235:125–130. https://doi.org/10.1016/j.synthmet.2017.11.013

Sworakowski J, Janus K (2017) On the reliability of determination of energies of HOMO levels in organic semiconducting polymers from electrochemical measurements. Org Electron 48:46–52. https://doi.org/10.1016/j.orgel.2017.05.031

Sworakowski J, Lipiński J, Janus K (2016) On the reliability of determination of energies of HOMO and LUMO levels in organic semiconductors from electrochemical measurements A simple picture based on the electrostatic model. Org Electron 33:300–310. https://doi.org/10.1016/j.orgel.2016.03.031

Tomasi J, Mennucci B, Cammi R (2005) Quantum mechanical continuum solvation models. Chem Rev 105:2999–3094. https://doi.org/10.1021/cr9904009

Ullah H, A-u-HA S, Ayub K, Bilal S (2013) Density functional theory study of poly(*o*-phenylenediamine) oligomers. J Phys Chem C 117:4069–4078. https://doi.org/10.1021/jp311526u

Ullah H, Shah HA, Bilal S, Ayub K (2014) Doping and dedoping processes of polypyrrole: DFT study with hybrid functionals. J Phys Chem C 118:17819–17830. https://doi.org/10.1021/jp505626d

Wu L-L, Luo J, Lin Z-H (1996) Spectroelectrochemical studies of poly-o-phenylenediamine. Part 1 situ resonance Raman spectroscopy. J Electroanal Chem 417:53–58. https://doi.org/10.1016/S0022-0728(96)04759-6

Yang S, Liao F (2012) Poly(p-phenylenediamine) nanofibers having conjugated structures, a novel, simple and highly selective fluorescent probe for l-cysteine. Synth Met 162:1343–1347. https://doi.org/10.1016/j.synthmet.2012.05.019

Yang L, Feng J-K, Ren A-M, Sun J-Z (2006) The electronic structure and optical properties of carbazole-based conjugated oligomers and polymers: a theoretical investigation. Polymer 47:1397–1404. https://doi.org/10.1016/j.polymer.2005.12.065

Yang S, Ye C, Song X, He L, Liao F (2014) Theoretical calculation based synthesis of a poly(p-phenylenediamine)–Fe_3O_4 composite: a magnetically recyclable photocatalyst with high selectivity for acid dyes. RSC Adv 4:54810–54818. https://doi.org/10.1039/C4RA11138A

Zoromba MS, Abdel-Aziz MH, Bassyouni M, Bahaitham H, Al-Hossainy AF (2018) Poly(o-phenylenediamine) thin film for organic solar cell applications. J Solid State Electrochem 22:3673–3687. https://doi.org/10.1007/s10008-018-4077-x